

SUMMARY OF DENSE HYDROGEN GAS FILLED RF CAVITY TESTS FOR MUON ACCELERATION *

K. Yonehara[#], M. Chung, M.R. Jana, M. Leonova, A. Moretti, A. Tollestrup, Fermilab, Batavia, IL 60510, USA

R.P. Johnson, Muons, Inc., Batavia, IL 60510, USA

B. Freemire, Y. Torun, P. Hanlet, Illinois Institute of Technology, Chicago, IL 60616, USA

Abstract

We show the recent analysis of a dense gas-filled RF cavity test by using a 400 MeV proton beam from Fermilab Linac. A large amount of RF power loading was observed in a gas-filled RF test cell when protons pass through the test cell. It can be explained that an ionized electron-ion plasma consumes RF power and transfers its kinetic energy to neutral gas molecules via the Coulomb interaction. We used several correction factors based on certain assumptions to evaluate the RF power consumption. The validity of these corrections and assumptions is discussed in this report.

PROTON INTERACTION WITH EXPERIMENTAL APPARATUS

Figure 1 shows the experimental apparatus. A 400 MeV proton beam passes through a collimator system and dense gas-filled RF test cell (TC). It is damped in a beam absorber. The TC is made of copper coated stainless steel. There is a pair of hemisphere copper electrodes to concentrate the RF field near the beam path. A 200 mm- ϕ 4 mm^h collimator hole is located in front of the TC to confine the beam in the TC. The beam current and profile are measured by using a toroid current transformer and a scintillating screen. The observed beam profile and simulated beam emittance from a beam lattice calculation are used to simulate the gas plasma distribution in the TC that will be discussed later. An induced RF field in the TC is measured by an RF pickup loop [1-3].

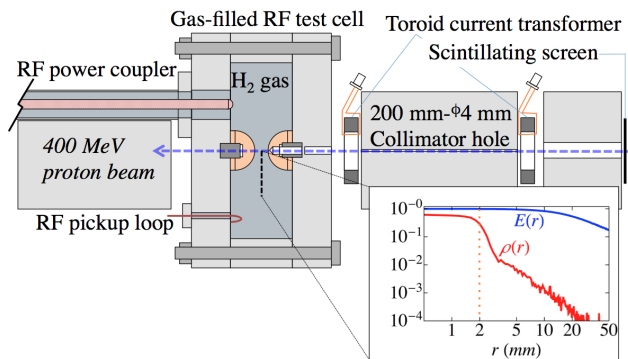


Figure 1: Whole layout of experimental apparatus and simulated radial distribution of electron-ion gas plasma in the TC and the normalized radial electric field distribution.

*Work supported by Fermilab Research Alliance, LLC under Contract No. DE-AC02-07CH11359 with the United States Department of Energy.

#yonehara@fnal.gov

Protons lose some of their kinetic energy before entering the RF field. Table 1 shows the average energy loss of protons in the various materials in which the protons pass through. Secondary particles are produced in the apparatus and air via the interaction between protons and materials.

The stopping range of electrons in air has been reported [4]. Low energy electrons ($K < 1$ keV) in air are eliminated from this analysis because their stopping range is very short ($\ll 1$ mm). On the other hand, a large number of delta rays ($K > 1$ keV) that are produced upstream of the collimator are eliminated by the collimator. A very small number of delta rays ($< 2 \cdot 10^{-4}$ e/p) can be produced in air and go through the beam monitor system. The yield of surface emission electrons [5,6] in the collimator hole is calculated. Although there are some uncertainties due to the details of geometric correlation between the beam angle and the material surface, the spectrum of surface emission electrons per proton is given $P(\epsilon) = c \times \epsilon(\epsilon + U_0)^{-(a+2)}$, where c is a constant, U_0 (~ 10 eV) is the work function of material, and a is the power of stopping power ($a \sim 4$). $P(\epsilon)$ is maximum at $\epsilon \sim 2$ eV and it is $\sim 10^{-9}$ at $\epsilon > 1$ keV. The overall effect of secondary electrons on the toroid current transformer and the scintillating screen is less than 1 %, which is negligible in the rest of analysis.

Table 1: Material, Thickness, Energy Loss and Initial and Final Kinetic Energies of a Proton Beam, Respectively

Element	Thickness	dK	K
Unit	mm	MeV	MeV
Initial			401.5
Ti-vacuum window	0.05	0.051	
Air	880	0.283	
Scintillating screen	1.00	0.814	
Air	400	0.129	
SS-beam window	3.18	5.56	
Cu electrode	3.18	5.99	
Final			388.2

Estimating the yield of gamma rays and its contribution in the TC is more complicated because high energy photons have long attenuation lengths in a material. We use *G4beamline* [7] to estimate the yield of gamma rays in our exact geometry. Table 2 shows the abundance of secondary particles in the TC. A large amount of high-energy gamma rays (> 10 keV) are produced in the

upstream apparatus from the TC via nuclear interactions. The cross-section of electron-production interactions of high-energy gamma rays with hydrogen is negligible (10^{-21} cm² or less). Photons in the middle energy range (100 eV to 10 keV) could also be produced via the Bremsstrahlung and K-shell electron capture processes. However, the production rates of such photons are negligible (See Table 2). Overall contributions of the photo-ionization process should be less than 1 %. It is reasonable to ignore all secondary particles except for secondary protons in the analysis.

Table 2: Simulated Yield of Secondary Particles in the TC: Values are Normalized by the Yield of Protons

Species	Yield
Proton (With the primary)	1.0
Gamma (All K)	0.73
Gamma (K < 10 keV)	$4.2 \cdot 10^{-5}$
Pion (+/-)	$8.0 \cdot 10^{-4} / 1.6 \cdot 10^{-4}$
Electron-Positron	$6.3 \cdot 10^{-4}$

The electron-ion pair production rate is estimated by using a formula,

$$\dot{N} = \dot{N}_b \times h \sum_k w_k \left(\frac{\rho_m dE/dx}{W_i} \right)_k \quad (1)$$

where h is the propagation distance, and w_k , ρ_m , dE/dx , and W_i are the abundance, mass density, stopping power, and effective average energy to produce single ion-pair [8] of the k -th gas molecule ($\sum_k w_k = 1$), respectively. The mass density of hydrogen is calibrated by using the Van der Waals equation. The correction factor is 7.5 % in 100 atm H₂.

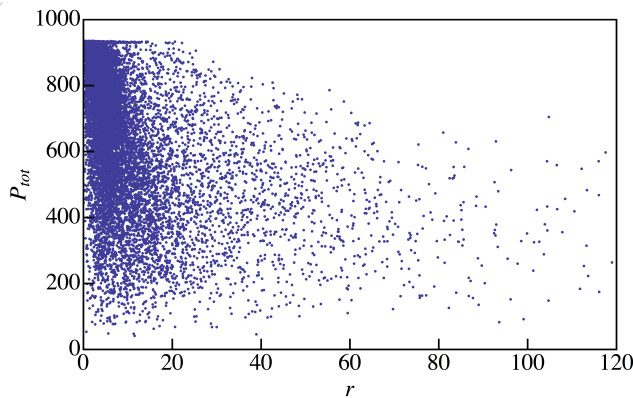


Figure 2: Total momentum (MeV/c) of protons in the TC as a function of radius (mm).

An accurate W_i is found in ref. 8. \dot{N}_b has a wide momentum distribution. It is determined from the beam current measurement and simulation. Figure 2 shows the simulated momentum distribution of protons in the TC as a function of radius. By using Eq. (1), we estimate the radial and longitudinal distribution of electron-ion plasma

per incident primary proton, $\rho(r, z)$ as shown in Fig. 1 (mid-plane of the TC).

ESTIMATED GEOMETRIC CORRECTION FACTOR

We represented the measured RF power consumption due to beam-induced plasma, dw at the peak RF electric field [1,2]. Actually, dw takes into account the gas plasma and electric field distributions. In this section, we show the geometric correction factor used to evaluate the measured dw .

The dw is analytically given by the following formula, $dw = \iiint 2\pi r \rho(r, z) (\mu_e + \mu_+) E(r, z)^2 \sin^2(\omega t) dt dr dz$, (2) where μ_e and μ_+ are the mobility of the electrons and positive ion in hydrogen gas, respectively. $E(r, z)$ is estimated using *SuperFish* [9]. There are measurements of μ_e and μ_+ as functions of gas pressure and electric field. Then, we can estimate the geometry correction factor for dw as

$$c_{geometry} = \frac{dw}{\mu_{e,+} E_{peak}^2}, \quad (3)$$

where E_{peak} is the peak RF electric field. $c_{geometry}$ is 0.66 for the electron swarm and 0.58 for the positive ion plasma.

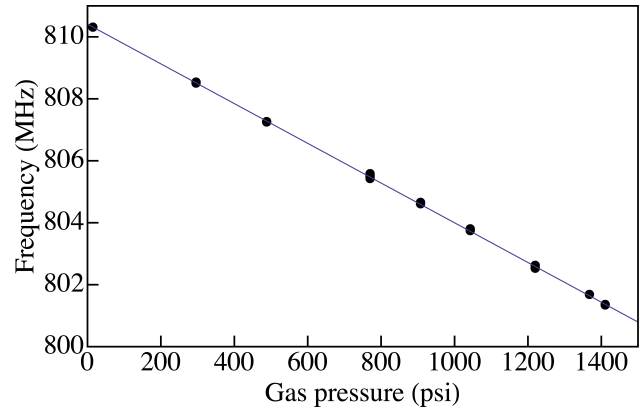


Figure 3: Observed resonant frequency as a function of gas pressure. Gas pressure is calibrated by the Van der Waals equation. The fit is $-0.0064 x + 810.409$, where x is gas pressure.

In order to estimate the RF stored energy in the TC, we calculate the capacitance of the TC, C_{TC} . *SuperFish* provides the RF stored energy, $\epsilon = 2.4 \cdot 10^{-4}$ Joules at $E = 1$ MV/m in 100 atm H₂ gas (frequency = 801.4 MHz). The gap between the two electrodes is 17.7 mm. Thus, C_{TC} is 1.53 pF ($C_{TC} = 2\epsilon/V^2$). C_{TC} is a function of resonant frequency, hence it is a function of gas pressure. It is worth noting that the capacitance correction also takes into account the possible deformation of the TC due to high gas pressure because we use the measured resonant frequency to estimate C_{TC} . Figure 3 shows the measured resonant frequency as a function of gas pressure in pure H₂ gas.

POSSIBLE SYSTEMATIC ERROR IN BEAM INTENSITY DEPENDENCE ON RF POWER LOADING MEASUREMENT

Figure 4 shows the measured dw in 20 atm H_2 gas at various electric fields ($E_{peak} = 5, 10, 18$ MV/m) as a function of beam intensity. First, the fluctuation of RF peak gradient is calibrated by using a power curve fit to dw as a function of X_0 where X_0 is the ratio between E_{peak} and the gas pressure. The residual of fit is within a few %. Then, the dw is averaged. That is the corrected dw .

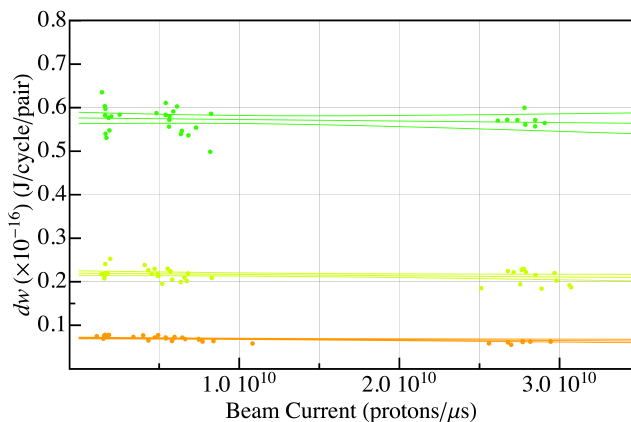


Figure 4: Measured dw vs Beam current. Gas pressure is 20 atm. The middle line in the set of lines is the best fit and other two correspond to a range of error with 3σ confidence level.

Figure 5 shows the deviation of measured dw at the lowest and highest beam intensities for various gas pressures. The measured dw tends to be low at high beam intensity in low gas pressure (negative deviation) and vice versa in high gas pressure (positive deviation). We define this deviation as a systematic error, which is 5~10 %.

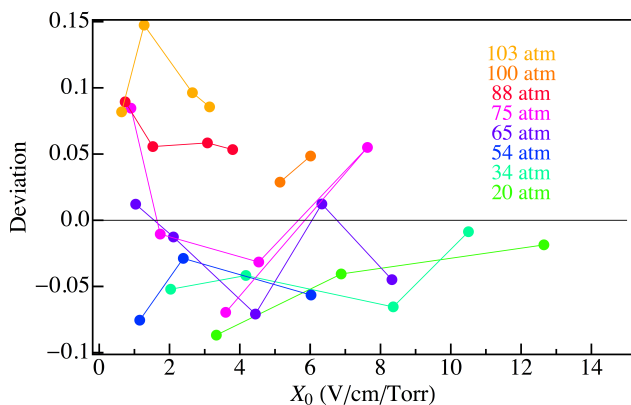


Figure 5: Plot shows the systematic error due to the beam intensity dependence.

Figure 6 is the corrected dw as a function of X_0 for various gas pressures. Each dw has an analysis error which involves the statistic and fit errors. It is typically a few %. The solid lines are the analytical dw that is estimated by using Eq. (2). The analytical dw is in good

agreement with the measured dw at low gas pressure. However, the measured dw has larger discrepancy at higher gas pressure and lower X_0 . It can be a gas pressure effect. We discuss the gas pressure effect in refs. [1,10,11].

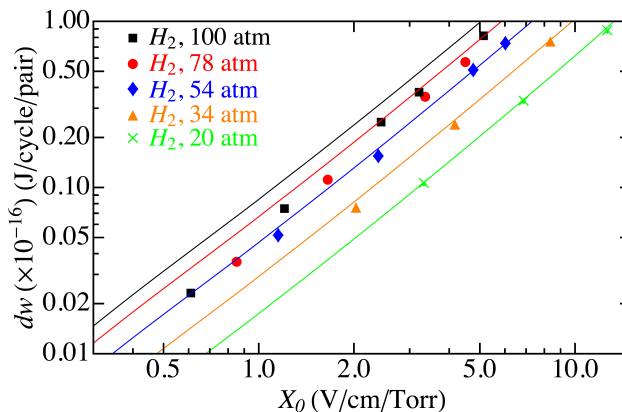


Figure 6: Corrected dw as a function of X_0 . The solid lines are a prediction from gas-plasma dynamics in RF fields [1, 2].

SUMMARY

We investigated the measured dw and evaluated its systematic error. The large systematic error was found in the beam intensity dependence. It is 10 %. On the other hand, the statistic error is very small, i.e. it is typically 2 ~ 3 %. The deviation of measured dw from the prediction is larger than any systematic and statistic errors. It means that the pressure dependence is real.

ACKNOWLEDGMENT

We thank to Vladimir Shiltsev and Mark Palmer for supporting this program. We also great thank to the Fermilab Accelerator Division, the safety group, and the beam operator for helping this experiment.

REFERENCES

- [1] B. Freemire, Doctoral Thesis at IIT, 2013.
- [2] K. Yonehara et al., IPAC12, MOPPC036, pp. 208.
- [3] M.R. Jana et al., IPAC12, MOPPR070, pp. 948.
- [4] A. Cole, Radiation Research 38, 7-33, 1969.
- [5] A.L. Hanson et al., J. Vac. Sci. Tech. A 19 (5) 2001.
- [6] P.H. Stoltz et al., Phys. Plasmas 13 056702, 2006.
- [7] T. J. Roberts, *G4beamline* (Muons, Inc. 2013), <http://www.muonsinc.com/muons3/G4beamline>.
- [8] C. J. Bakker and E. Segre, Phys. Rev. 81 489 (1951).
- [9] R.F. Holsinger and K. Hlbach, *SuperFish* (LANL), http://laacg1.lanl.gov/laacg/services/download_sf.html#ps1.
- [10] K. Yonehara et al., Proceedings of IPAC13, TUPFI058.
- [11] B. Freemire et al., Proceedings of IPAC13, TUPFI064.